

# Direct fabrication of seamless roller molds with gapless and shaped-controlled concave microlens arrays

Guangqing Du,<sup>1</sup> Qing Yang,<sup>1,2</sup> Feng Chen,<sup>1,\*</sup> Hewei Liu,<sup>1</sup> Zefang Deng,<sup>1</sup> Hao Bian,<sup>1</sup>  
Shengguan He,<sup>1</sup> Jinhai Si,<sup>1</sup> Xiangwei Meng,<sup>1</sup> and Xun Hou<sup>1</sup>

<sup>1</sup>State Key Laboratory for Manufacturing Systems Engineering and Key Laboratory of Photonics Technology for Information of Shaanxi Province, School of Electronics and Information Engineering, Xi'an Jiaotong University, Xi'an 710049, China

<sup>2</sup>e-mail: yangqing@mail.xjtu.edu.cn

\*Corresponding author: chenfang@mail.xjtu.edu.cn

Received July 6, 2012; revised September 4, 2012; accepted September 17, 2012;  
posted September 18, 2012 (Doc. ID 172131); published October 19, 2012

This Letter demonstrates the direct fabrication of gapless concave microlenses on glass cylinders, which can be used as seamless roller molds for the continuous imprinting of large-area microlens arrays. The method involves femto-second laser exposures followed by a chemical wet-etching process. A honeycomb-like concave microlens array was fabricated on a glass cylinder with a diameter of 3 mm. We demonstrated the flexibility of the method in tuning the shape and depth of the concave structures by the arrangements of the laser exposure spots and laser powers, and examined the replicating ability of the roller mold by the polymer casting method. © 2012 Optical Society of America

OCIS codes: 140.3330, 140.3390.

The large-area microlens arrays (MLAs) have found potential applications in the fields of light extractions and brightness enhancement films used in the light-emitting devices and flat-panel displays [1,2]. Among the emerging techniques for fabricating the large-area MLAs [3–5], roller imprinting clearly stands out as one of the best choices because of the superiority of its cost-efficiency, high-resolution, and easy-manipulation. But a major road-block has remained for this technology: fabrication of the high-quality rolling molds. For continuous imprinting of convex refractive microlenses, high-quality rolling molds require the needed concave microstructures to be fabricated seamlessly on the cylindrical surfaces, and the materials, commonly metals and glasses, should be durable enough for the continuous imprinting. The current processes for fabricating roller molds, however, are difficult to meet above requirements. For example, some simple approaches such as wrapping the flat sheets with microstructures on cylinders and soft lithography cannot remove the seams on the rollers, and the materials are soft and unstable; direct machining on metallic rollers using the diamond cutters, lasers, and cylindrical photolithography process can produce seamless patterns on hard materials, but it suffers such drawbacks as long processing time, poor profile controllability, and the rough surfaces [6–10].

The motivation of this Letter is to overcome the current challenges of seamless roller molds. We proposed a femtosecond laser-enhanced chemical etching process to directly fabricate gapless microlens arrays on silica glass cylinders [11]. The current procedures can be used to fabricate concave lenses on nonplanar substrates, which is essentially innovative for fabrication of seamless roller molds for high efficiency and continuous imprinting of large-area MLAs. This method does not require complicated top-down procedures of the conventional laser ablation techniques [12,13], and thereby it promotes the processing speed by at least one or two orders of magnitude. The debris-free process also guarantees the smoothness of the fabricated concave

microlenses. Because the applicable materials, such as glass, fused silica, and quartz, are transparent and durable, the fabricated roller molds can be used in both mechanical embossing and ultraviolet curing imprinting technologies [6,14]. Additionally, the maskless process enables facile control of the dimension and shape of microstructures on the cylindrical surfaces.

We demonstrated the ability to create the seamless roller molds with gapless microlens arrays by fabricating a honeycomb-like concave microlens array on the annularity of a silica glass cylinder with a diameter of 3 mm (Fig. 1). The array is composed of 5400 hexagonal-shaped microlenses, and the diameter of each lens is about 60  $\mu\text{m}$ . The structures were achieved within two  $h$ . From the SEM observation as shown in Fig. 1(b), the microlenses are gapless packed with clear and sharp boundaries. Figures 1(c) and 1(d) demonstrate the uniformity and smoothness of the fabricated microlens array. The average surface roughness value,  $R_a \approx 10$  nm, which was tested in an area of  $15 \mu\text{m} \times 15 \mu\text{m}$  at the bottom of a concave structure. The nanometer-scaled surface roughness is essential for the optical devices, such as microlenses, to reduce the light scattering and

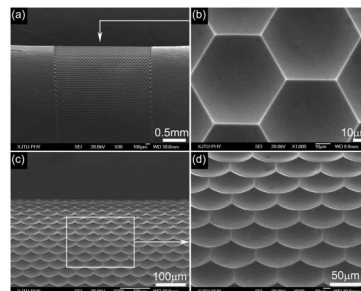


Fig. 1. SEM observations of the microlens array. (a) Overall observation of the microlens array. (b) Magnified top view of the microlenses on the cylindrical surface. (c) Side view of the microlens array. (d) Magnified side view of the microlens array.

achieve high-resolution imaging performances, but fabrication of smooth surfaces is still challenging for the laser ablation and mechanical milling processes.

To fabricate the concave MLA on the glass cylinder, a laser-based two-step method was used, which is schematically depicted in Fig. 2(a). We started with a point-by-point laser exposure process to create an array of photon-modified spots on the cylindrical surface using a train of 800 nm, 30 fs laser pulses with a repetition rate of 1 kHz. In the experiment, 3.5 mW laser pulses were focused by an objective lens (N.A. = 0.5) and the exposure time for each spot,  $t = 500$  ms [15], which was controlled by a mechanical shutter. To create the cylindrical-distributed laser exposure spots, the sample was coaxially connected with a rotation stage by a high-precision tap chuck, which was mounted on a three-dimensional (3D) translating stage [Fig. 2(b)]. By alternately translating and rotating the sample in the axial ( $x$ -direction) and circumferential direction, triangle-arranged exposure spots were generated on the glass cylinder [Fig. 2(a)]. To guarantee the equal conditions of the laser exposures, the offsets of the focal plane during the sample rotating and translating shall be minimized. Two methods were adopted: (1) the concentricity between the chuck and the rotation stage was accurately revised, decreasing the offset of the sample surface to  $<5$   $\mu\text{m}$ , and (2) a CCD camera was used to monitor the laser exposure process, which can be stopped to be revised when the focal spot of the laser pulses deviate from the sample surface. To achieve the seamless pattern, the exposure spots were equidistantly distributed on the cylindrical surface (the rotation angle of each step was 2 deg), and thereby the line distance along the circumferential direction,  $l$ , was about 52.3  $\mu\text{m}$ . The interspacing between two spots along the axial direction,  $d = 2l/\sqrt{3}$  was about 60.39  $\mu\text{m}$ . We created an array of 5400 ( $30 \times 180$ ) exposure spots, which took about 1 h. After the laser exposures, the glass cylinder was treated by 5% diluted hydrofluoric (HF) acid solution for 45 min at the room temperature. The chemical etchings were significantly enhanced in the laser-modified areas, generating circular-shaped concave structures. The morphology evolutions of the sample surface were captured by the

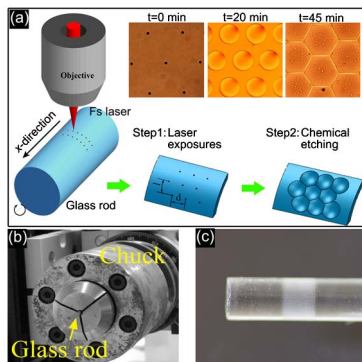


Fig. 2. (Color online) (a) Schematic diagram of the fabrication process. The insert figures show the morphology revolutions of the exposure spots during the chemical etching process. (b) Optical image of the tap chuck. The glass rod was fixed in the chuck. (c) Optical profile of the glass rod with the fabricated microlens array.

CCD camera, as shown in the insertions of Fig. 2(a). The diameters of these microstructures were increased with the chemical etchings and consequently overlapped with each other, forming the honeycomb-like pattern [Fig. 2(c)].

The self-formation of the concave microstructures in the chemical etching process can be used to contribute to the femtosecond-laser-induced material modifications, which significantly enhance the chemical etching velocity. In the laser-glass interactions, the absorption of photon energy through the multiphoton ionization and avalanche ionization triggers microexplosions, and builds up a strong pressure that can reach a scale as high as TPa [16]. This pressure extremely exceeds Young's modulus of cold glass ( $\sim 75$  GPa), which causes the modifications of materials, such as phase transitions, densification, and the reduction of Si-O-Si bond angle [16,17]. Consequently, the modified materials were chemically etched out by the HF acid solutions with slight damages on the original materials, forming the smooth concave microstructures (Fig. 1).

To demonstrate its flexibility in controlling the shape of the structures, a complex concave MLA with pentagonal- and hexagonal-shaped microlenses was fabricated on the glass cylinder [Fig. 3(a)]. Other microlens arrays with different shapes and sizes can be fabricated with different arrangements of the laser exposure spots. At the same time, the depth of the concave microstructures can be tuned by the laser powers. We investigated the power dependency of the depths by exposing the glass surface with different laser powers ranging from 0.5 mW to 4.5 mW. After the 45 min HF (5% diluted solution) treatments, concave microstructures were fabricated. We measured the depths of the structures by a laser confocal microscope and plotted the results in Fig. 3(b). It indicates that the depths increased from  $\sim 4$   $\mu\text{m}$  to  $\sim 20$   $\mu\text{m}$  with increasing laser power, and the increasing trends slowed down when the power exceeds 4 mW. For the gapless MLAs, as discussed, the shape and size of the structures are determined by the arrangements and intervals of laser exposure spots, respectively. Therefore, combined with the power dependency of the depth, the curvature radii of the microlenses, determined by the diameters and depths, can be tunable by the arrangements of laser exposure spots and powers.

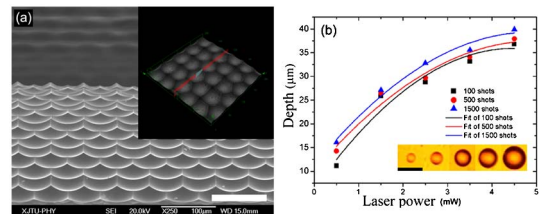


Fig. 3. (Color online) (a) SEM images of the microlens array on the glass cylinder, which is composed of pentagonal and hexagonal-shaped lenses. Two scale bars denote for 100  $\mu\text{m}$ . (b) Power dependency of the depth of the concave microstructures. Triangles, dots, and blocks denote the different exposure times, which are 1500, 500, and 100 ms, respectively. The insertion shows optical profiles of the concave structures. The scale bar equals 100  $\mu\text{m}$ .

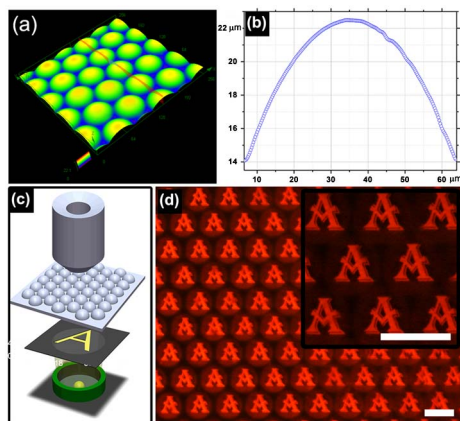


Fig. 4. (Color online) (a) Part of 3D profile of the convex microlens array that was replicated from the roller mold. (b) Cross-sectional profile of a microlens in the replica. (c) Optical setup for testing the imaging property of the microlens arrays. (d) Images of the letter A. Scale bars denote 100 μm.

Except for the roller molds, rolling imprinting of large-area MLAs requires a complicated mechanical system. In this work, we examined the replicating ability of the fabricated seamless roller mold by an alternative approach. We dipped the glass cylinder with the hexagonal-shaped concave microlens array in the liquid poly (dimethylsiloxane) [PDMS] and heated the sample at 75°C for 30 min. After the PDMS was cured, we peeled off the polymer thin film with convex microlenses replicated on it. The 3D and cross-sectional profiles of the MLA were measured by the laser confocal microscope, as shown in Figs. 4(a) and 4(b). The diameter and height of the microlens are 61.6 μm and 8.5 μm, respectively. The focal length of the microlenses can be calculated according to  $f = (R^2 + h^2)/2h(n - 1) - h(n - 1)$ , where  $R$  and  $h$  are the radius and height of microlenses, respectively, and  $n$  is the refractive index of PDMS. Given  $n = 1.51$ , we get  $f = 113.4$  μm. The imaging property of the replicated MLA was tested by an optical microscope system [Fig. 4(c)]. Clear images of the letter A were captured by the CCD camera, as shown in Fig. 4(d), demonstrating the nanoscaled surface smoothness and excellent cross-sectional profiles of the microlenses. The imaging quality of the imprinted MLAs through the roller molds is obviously superior than that of the microlenses obtained by laser direct writing [13], benefiting from the chemical polishing process, in which the surface roughness can be reduced to as small as 20 nm.

We proposed a femtosecond-laser-induced chemical process to fabricate concave microstructures on glass cylinders. A honeycomb-like concave MLA, which is

composed of 5400 lenses, was fabricated on a glass cylinder, and its replicating ability was also examined by a simple PDMS casting method. The advantages of this technique, such as the ability to create seamless roller molds with nanometer surface roughness, facile and highly efficient fabrication procedures, and ease of tuning the shape and size of microlenses have been demonstrated in the experiments. The presented method can be used in highly precise fabricating complex 3D microstructures on curved substrates and promotes large-area and low-cost imprinting of 3D microstructures.

This work is supported by the National Science Foundation of China under the Grant No. 61176113, National High Technology Research and Development Program of China under the Grant No. 2009AA04Z305, and the Fundamental Research Funds for the Central Universities.

## References and Notes

1. J. P. Yang, Q. Y. Bao, Z. Q. Xu, Y. Q. Li, J. X. Tang, and S. Shen, *Appl. Phys. Lett.* **97**, 223303 (2010).
2. M.-K. Wei and Su I-Lin, *Opt. Express* **12**, 5777 (2004).
3. C.-P. Lin, H. Yang, and C.-K. Chao, *J. Micromech. Microeng.* **13**, 775 (2003).
4. D. L. MacFarlane, V. Narayan, J. A. Tatum, W. R. Cox, T. Chen, and D. J. Hayes, *IEEE Photon. Technol. Lett.* **6**, 1112 (1994).
5. J. Yao, J. Q. Su, J. L. Du, Y. X. Zhang, F. H. Gao, F. Gao, Y. K. Guo, and Z. Cui, *Microelectron. Eng.* **53**, 531 (2000).
6. S. H. Ahn and L. J. Guo, *Adv. Mater.* **20**, 2044 (2008).
7. A. M. Bowen and R. G. Nuzzo, *Adv. Funct. Matter.* **19**, 3243 (2009).
8. A. Y. Yi and L. Li, *Opt. Lett.* **30**, 1707 (2005).
9. W. Wang, X. Mei, and G. Jiang, *Int. J. Adv. Manuf. Technol.* **41**, 504 (2009).
10. Y.-C. Lee, H.-W. Chen, and F.-B. Hsiao, *J. Microelectromech. Syst.* **21**, 316 (2012).
11. F. Chen, H. Liu, Q. Yang, X. Wang, C. Hou, H. Bian, W. Liang, J. Si, and X. Hou, *Opt. Express* **18**, 20334 (2010).
12. D. Wu, S.-Z. Wu, L.-G. Niu, Q.-D. Chen, R. Wang, J.-F. Song, H.-H. Fang, and H.-B. Sun, *Appl. Phys. Lett.* **97**, 031109 (2010).
13. H. Liu, F. Chen, X. Wang, Q. Yang, D. Zhang, J. Si, and X. Hou, *Opt. Commun.* **282**, 4119 (2009).
14. J.-T. Wu and S.-Y. Yang, *J. Micromech. Microeng.* **20**, 085038 (2010).
15. A long exposure time will help to fabricate uniform concave structures, but sacrifice the processing efficiency. And the used value of 500 ms is an optimized result in the previous experiment shown in Chen *et al.* [11].
16. H. Feng, X. Wang, and H. Zhai, *J. Phys. D* **44**, 135202 (2011).
17. E. G. Gamaly, S. Juodkazy, K. Nishimura, H. Misawa, B. Luther-Davies, L. Hallo, P. Nicolai, and V. T. Tikhonchuk, *Phys. Rev. B* **73**, 214101 (2006).